Check for updates

Experimental determination of metals generated during the thermal failure of lithium ion batteries†

Jonathan E. H. Buston, iD * Jason Gill, iD Rebecca Lisseman, Jackie Morton, iD Darren Musgrove and Rhiannon C. E. Williams

Lithium ion cells, although near ubiquitous as a portable power source in today's society, have rare, but well documented failure pathways which generate gas, fumes and smoke, and often result in fire. Whilst the composition of the gas has been subject to much analysis, far fewer reports have focussed on the nature of any solid materials released. This work describes the causing to fail (by applying an external heat source) of a range of commercially available and widely used cells. Samples of both the smoke generated during the failure, and the residues left surrounding the cell after failure, were analysed for metal content by ICP-AES. These showed that all samples contained the key metals expected to be in cell cathodes (nickel, manganese, cobalt and aluminium) in not dissimilar ratios. However, the ratio of these elements differed from cell to cell, as the cathode varied.

Broader context

Lithium ion batteries currently play a dominant role in energy storage, particularly at a smaller scale. Current generations of lithium ion batteries most often use cathodes containing lithiated nickel, manganese and cobalt oxides. Similar materials are known to be human carcinogens. Whilst accepted by consumers, there have been events which are caused by, or involve, these batteries catching fire. Once failing, or on fire, lithium ion batteries can emit a range of substances, including gases and metal particulate as near-field residue. The gases generated have been studied, and a few reports have sampled the near-field residue. However this study is the first to investigate the metal content of the white smoke generated by failing lithium ion batteries, and compare the composition of the smoke to the near-field residues ejected from the burning batteries. We have shown that nickel, cobalt and manganese are present in the smoke as well as the near-field residues, and are in similar ratios to those expected from the cathodes within these batteries.

Introduction

Lithium ion batteries are widespread in society and are an essential component of the global drive to reduce carbon emissions. Smaller batteries are used to power portable consumer electronics; larger battery packs are utilised in the electric vehicles (EV) driving low carbon mobility and in Battery Energy Storage Systems (BESS). Such large storage systems typically contain many tonnes of lithium ion cells and are fundamental in supporting the transition to renewable energy generation, impacting power quality (enabling stabilisation of the electricity supply frequency when clouds or wind gusts disturb generating capacity) and time shifting the generated capacity to meet demand. However, new technology brings new

HSE Science and Research Centre, Harpur Hill, Buxton, Derbyshire, SK17 9JN, UK.
E-mail: jonathan.buston@hse.gov.uk

risks that need to be managed. Lithium ion batteries and fires relating to lithium ion batteries at all scales have been well reported both in the scientific literature (for example, for consumer electronics the Galaxy Note incidents;[1] for EVs[2,3] and for BESS[4]) and indeed, by popular reports on social media.[5]

These failures are most often the result of a self-accelerating process known as thermal runaway and can be initiated by a myriad of causes *e.g.*, internal short circuits, physical damage[6] or being subjected to heat from an external source (including an external fire).[7,8]

The outcome of a thermal runaway process in a lithium ion battery is the generation of excess heat leading to thermal break down of the cell components and the production of a mixture of gases within the cells. The cells are eventually unable to contain the gas generated (which is subsequently liberated by venting). In broad terms, this gas is typically a flammable mixture of hydrogen, carbon dioxide, carbon monoxide (if an unignited event) and some hydrocarbons[9–11] (with traces of many other compounds[12]). The presence of carbon monoxide and traces of

hydrogen fluoride also give this gas mixture a level of toxicity. In most cases this gas will be ignited immediately (components from the failing cell can act as an ignition source). However, depending on the release scenario, a delayed ignition, or no ignition may occur. Possible consequences for a cell failure fire event are: the production of jet flames (from the directional release of flammable gas); the ejection of the contents of the cell (either as particulate matter or as significant parts of the cell); and the production of combustion gases and fume. A further scenario is the propagation of the event through a battery pack as the excess heat generated by one cell failing causing neighbouring cells to enter thermal runaway,[13] escalating in the worst case to full pack failure.

There is a body of work which has investigated the combustion gases produced by cell failure.[12,14–16] However, as cell technology advances, in order to achieve goals such as increased energy density, the "chemistry" (the composition of the anodes, cathodes and electrolytes) within a lithium ion cell are being developed to enable this. As a result, ongoing work is needed to validate that any prior assumptions about gas compositions remain valid. The particulate dust ejected from the cells has been investigated by Zhang,[17,18] Chen,[19] Essl[20] and Wang.[21] Each of these groups collected the dust from within a confined chamber and showed that proportions of the dust contained not only carbon-based materials from the cell anode, but metal containing particles from the cell cathode. Other work has investigated the residues collected from a fire from an EV battery pack within a tunnel,[22] and investigated the clean-up remediation needed.[23] Very recently a report by Barone[24] investigated the aerosols emitted from three different lithium ion cells, demonstrating that the aerosol contained materials deriving from the cell electrodes.

There has been no report to date on the composition of the much finer particulate matter carried as the smoke from a battery fire. These finer particles are more likely to be inhaled or ingested by bystanders, first responders, and those clearing up after an event.

As lithium ion cells fail, most often the first indication is the release of a white smoke containing vent gases,[9] particulate matter and possibly aerosolised electrolyte droplets. For many cells, and in many circumstances, this mixture self-ignites to produce a fire, although this is not inevitable.

When lithium ion battery fires occur, they are often characterised by the production of white smoke. In the case of a battery undergoing thermal runaway that has not yet produced a fire event the smoke is white in appearance.[25] If the battery does not produce flame, due to lack of ignition source, or lack of oxygen to sustain combustion, it can form a dense white cloud. This has been observed during some notable recent events, for example the BESS fire in Belgium[26] and the BESS explosion at the McMicken facility in Arizona (2019).[27,28]

The release of such a cloud of smoke is a risk in terms of potential exposure to hazardous materials and any subsequent impact on health such an exposure could have. Therefore, in order to assess battery smoke exposure it is necessary to analyse and characterise the content of such emissions. The smoke is

likely to contain a range of plasticisers from casings, acid and organic gases, volatile organic compounds as well as metals from the battery compartment. Whilst there have been studies published relating to the composition of gases produced by lithium ion cells when they fail, there has been no investigation of the non-settling particulate matter in the smoke, although a Tesla Emergency Response Guide does refer to "oxides of carbon, nickel, lithium, copper, and cobalt".[29]

The main metals that are found in the secondary (rechargeable) batteries as tested here are aluminium, cobalt, manganese and nickel as well as lithium. There are of course other trace elements that may be present. There are also further associated hazards not discussed here including the emission of hydrogen fluoride[8] and organic compounds such as benzene and toluene.[30]

Airborne metal particles produced as a result of battery combustion will be composed of a variety of elements (and compounds containing them) at a range of concentrations and particle size which will alter both bioavailability and overall toxicity. For instance, smaller inhaled metal particles will deposit deeper within the lung than larger particles. In addition, residence time varies with some metals exhibiting long residence times in lungs and airways whilst other metal species, once inhaled can be quickly distributed around the body. Residence and translocation times are affected by properties such as charge, surface reactivity, solubility, hydrophobicity or polarity, agglomeration state, and the ability to interact with biological tissue and generate reactive oxygen species, all of which are important determinants of toxicity.[31]

Metal residues must also be considered as a source of exposure following a battery release; potential routes of exposure could occur through both dermal uptake and any inhalation or ingestion of metals as a result of direct or indirect transfers.

Each metal determined in this study has its own associated hazard. Nickel and cobalt are known sensitisers, both are known to cause respiratory issues including 'asthma like' allergic reactions. In addition, nickel and nickel compounds are classified Group 1 carcinogens as defined by IARC and nickel can cause skin irritation and allergic dermatitis at sometimes low concentrations.[32] Elevated exposure to cobalt can affect heart, thyroid, liver, and kidneys. Repeated exposure to cobalt dust can cause scarring of the lungs (fibrosis) even if no symptoms are noticed. Aluminium compounds have been linked to asthma, obstructive pulmonary disease, and heart disease, however it is better known for causing adverse neurological effects.[33] With manganese compounds the central nervous system is the primary target of manganese toxicity, specifically causing detrimental neurological effects, since inhaled manganese is often transported directly to the brain before it is metabolised by the liver.[34,35] People are exposed to lithium inadvertently from drinking water supplies as a result of the cycle of pharmaceuticals (as a treatment for bipolar and depression) entering environmental systems. Inhalation exposures can cause a burning sensation, a cough, shortness of breath, sore throat and eyes if not protected can cause pain,

burning and redness. Ingestion can cause abdominal cramps, burning sensations, nausea, shock or collapse and weakness.[36]

The aim of this project was to capture and analyse smoke released when a lithium ion battery is allowed to burn in air. The batteries investigated consisted of range of commercially available cells that were expected to have a range of different cathode "chemistries" – that is range of metal oxides ranging from lithium cobalt oxide (LCO, $LiCoO_2$) to the mixed lithium nickel manganese cobalt materials (NMC, $LiNi_xMn_yCo_{(1-x-y)}O_2$) and lithium nickel aluminium oxide (NCA, $LiNi_{0.8}Co_{0.15}Al_{0.05}O_2$). We aim to investigate the metals composition of the smoke particulate, comparing it to the solid residue exuded from the cells during failure to investigate if any particular species is prone to being more concentrated within the smoke.

Test strategy

For this initial study failure was induced in a range of fully charged, cylindrical, lithium ion cells by the application of external heat. This was sufficient to initiate a thermal runaway event. The test enclosure was designed with sufficient volume to provide enough oxygen to support complete combustion. Since these failures were often characterised by violent combustion, no attempt was made to completely confine the event to quantify all the gas and smoke products. Instead, a semi-confined enclosure was used, and the smoke sampled from the enclosure chimney (Fig. 1). In addition, the residues deposited outside the cell within the test enclosure were sampled.
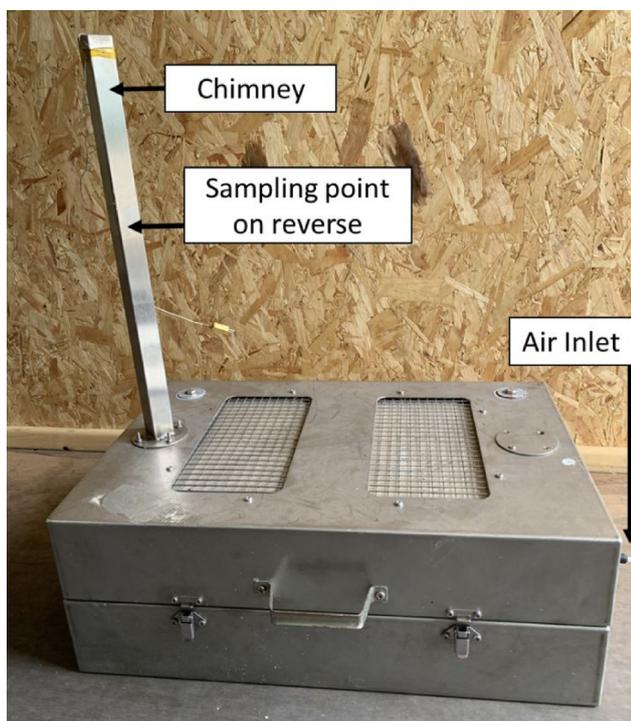

Fig. 1 Test Enclosure.

All of these samples were analysed for the presence/and relative quantification of the key metals expected to be present in the cells.

Test method

The test enclosure

The test enclosure ($600 \times 400 \times 220$ mm, internal volume approximately 50 litres, Fig. 1) was constructed from stainless steel (2 mm thick) and lined within with an insulation board (Pressphan mica 1 mm thick). This lining was changed between each test to ensure fresh sampling surfaces. A chimney (25 mm square) was fitted to the top of the enclosure; partway up the chimney was a port for the particulate sampling filter (25 mm Whatman QM-A quartz filters). Air was drawn through this filter by a dedicated sampling pump at 2 litres per minute. Due to the rapid increases in gas volumes expected, the filter did not attempt to sample all the smoke particulate generated. Make-up air was supplied to the enclosure at a rate of just over 2 litres per minute. The enclosure was equipped with an internal camera and light.

The volume of the enclosure was sufficient to ensure that the completeness of the combustion process was not limited by oxygen availability. We have previously demonstrated that the failure of a 5 A h NMC cell consumes approximately 7 litres of oxygen (33 litres of air).[37] Of course, the completeness of the combustion is dependent on several factors; the dynamics of combustion (including that of any gases vented from the cell prior to the ignition) are important as well as the bulk availability of oxygen. However, we wished to not place an artificial limit on the combustion by inadvertent use of an undersized enclosure.

The test procedure

Each cell was prepared by firstly charging to 100%. Then a thermocouple (Type K) and an electric cartridge heater (200 W at full power, 3/8" diameter, 1.5" long) were attached (Fig. 2). The cell was then placed within the enclosure and held in position by a further restraining wire.

The enclosure was placed within the HSE SRC abuse testing facility, with ventilation, video recording, and datalogging systems (data recorded at 1 Hz for these tests). The test was initiated and monitored remotely from the control room (15 m
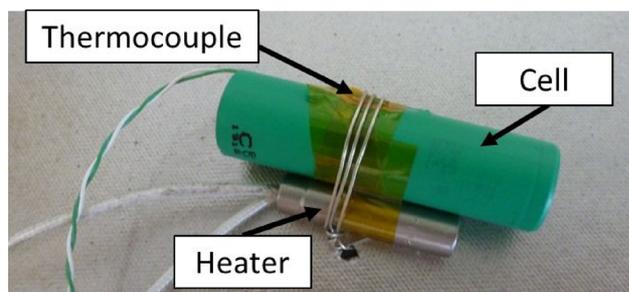

Fig. 2 A cell prepared for testing.

from the abuse chamber). Initiation was caused by applying a voltage to the heater until the cell had failed. After the test event had completed and allowing time for the atmosphere within the chamber to be purged, the enclosure was opened, photographed, and several surface swabs (Ghost Wipes, 150 × 150 mm, environmental express) taken from the inside of the enclosure; one from an area of apparently heavy contamination, the other from a less obviously contaminated area, each taken within a 100 × 100 mm grid.

Analysis of the residues

Analysis of both the filters and swap samples was performed by first digesting the sample materials (3 ml HNO_3/2 ml HCl/ 0.25 ml HF at 95 °C for 1 hour in a graphite heating block) as per BS ISO 15202-2:2012 Workplace air – determination of metals and metalloids in airborne particulate matter by inductively coupled plasma atomic emission spectrometry (ICP-AES) Part 2: (sample preparation). Following dilution of the digest, subsequent analysis as performed by ICP-AES (as per BS ISO 15202-3:2004 workplace air – determination of metals and metalloids in airborne particulate matter by inductively coupled plasma atomic emission spectrometry Part 3: analysis).

Cells tested

Within this paper, nine different cells from seven manufacturers were tested. These are all commercially available 18 650 sized cells and assumed, in good faith, to be genuine. These cells were selected to be representative of the market, in terms of capacity, manufacturer and the lithium ion chemistry. Lithium iron phosphate cells were not investigated in this work.

Both the nameplate and measured capacity of each cell type are shown in Table 1, together with their nominal voltage, and indication of cell chemistry, where available from the datasheet. The measured capacity of a sample from cell type was determined by taking two cells from each batch which were cycled twice at 1 A charge/discharge and once at 0.5 A charge/ discharge. A standard constant current–constant voltage (CCCV) protocol was used across each cell-charging to 4.2 V, 50 mA cut-off and discharging to 2.75 V. The reported values are the average of these cycles, giving a real-world capacity. The measured internal resistance is the average of these two cells post cycling.

All cells were charged to 100% state-of-charge for this work.

Results

When external heat was applied, all the cells tested vented gas and smoke and self-ignited to produce a flame. In most cases, this venting was a violent event, accompanied by flame, observed by the camera within the test box. In some tests, smoke and/or flame were observed venting from other places on the box (Fig. 3). This is an indication of the rapidity of the venting. For the purposes of these experiments, no attempt was made to seal all exit paths from the test box.

A summary of each of the cell failure events is given in Table 2.

Typically, the temperature on the surface of the cell rose rapidly as the cells entered thermal runaway; the air temperature within the test box and its chimney also rose when flame/ combustion events occurred; a typical example is shown in Fig. 4 (cell D).

After the cell failed, the test box was left to cool, and then further examined. It was seen that venting had occurred from the relief point designed into the top (positive terminal) end of the cells. This venting often gave rise to a patterned spread of a dark ejected residue, Fig. 5. Swabs were taken both of an area obviously contaminated, and of an area not covered by the darker residue.

The filters which sampled the smoke fume, and the residue swabs from inside the chamber and the cell after ignition and cool down, were analysed for a range of metals commonly expected to be within a lithium ion cell. The metals determined were aluminium, cobalt, copper, iron, lithium, manganese and nickel; lithium, nickel, manganese cobalt and aluminium are likely (in some combination) to form the active cathode material of a cell, coated onto an aluminium foil "current collector", the anode is most generally carbon, coated onto copper foil current collector, and there will be lithium within this. The cell casings are most generally made from nickel coated steel; this could provide a source of low levels of nickel even if the cathode material is not nickel containing.

Fig. 6 shows a graphical representation of the relative proportion of metal concentrations for the analysis undertaken when cell C was heated in the chamber, with the proportions given in Table 3.

The MSDS of this cell names the cathode material as "Lithium nickel manganese cobalt oxide" (without giving the proportions of the metals). It can be seen that all the metals expected to be within the cell are seen within the collected

Table 1 Commercially available 18650 cells used in this study

Cell	Nominal capacity mA h	Actual capacity mA h	IR mΩ	Nominal voltage	Cathode chemistry, where known
Cell A	2600	2530	45	3.7	"Based in lithiated metal oxide (Cobalt, Nickel, Manganese)"
Cell B	3250	3180	35	3.6	
Cell C	1750	1710	14	3.6	"Lithium nickel manganese cobalt oxide"
Cell D	2600	2520	44	3.6	
Cell E	3200	2840		3.7	
Cell F	2450	2440	40	3.7	
Cell G	2350	2410		3.7	Lithium cobalt oxide (LCO)
Cell H	2200	2030	18	3.62	
Cell I	2200	2090	42	3.6	

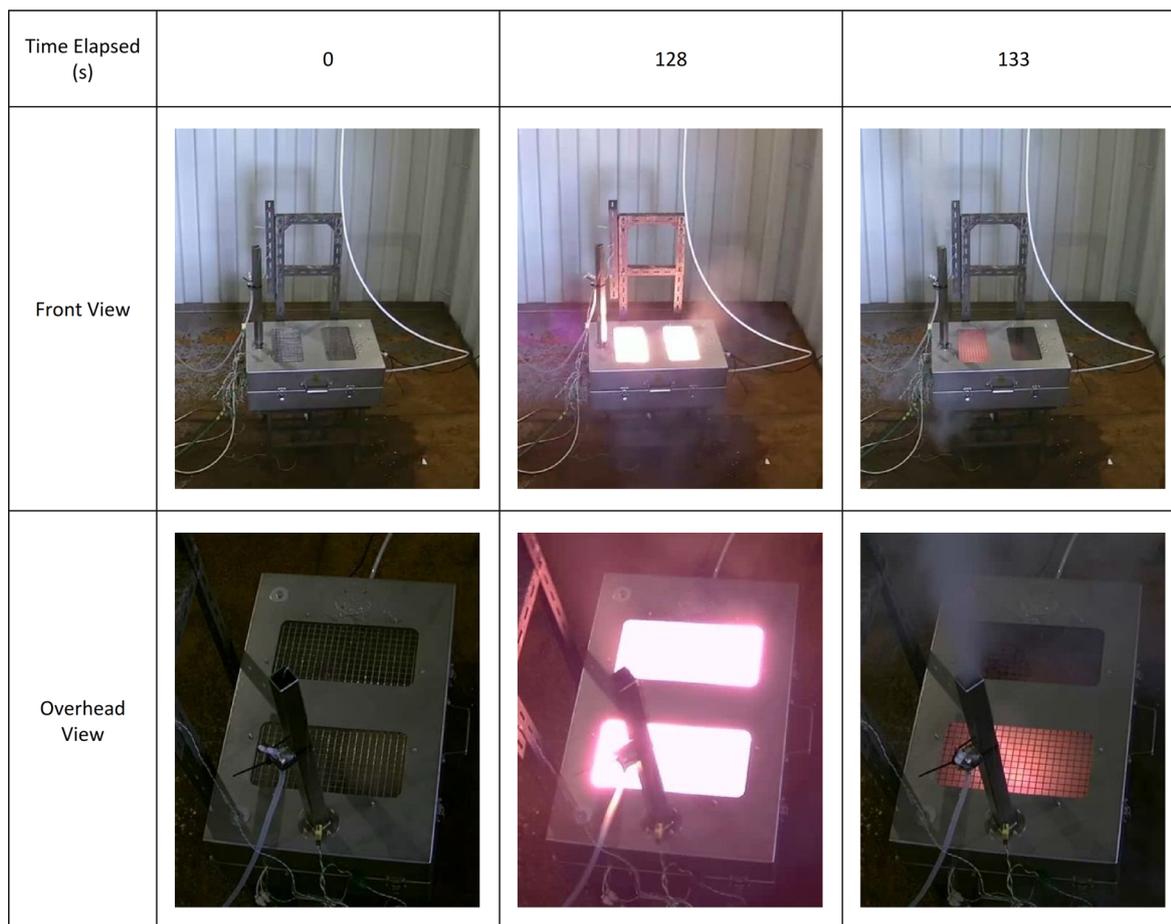| Time Elapsed (s)	0	128	133
Front View			
Overhead View			

Fig. 3 Event for cell A.

Table 2 Timeline and outcome of cell failure events

Cell	Time of heating to vent (s)	Peak cell surface temp (°C)	Description of event
Cell A	128	773	Cell vented gas and electrolyte, then an initial flash flame event which rapidly subsided, flowed by a second flame event 5 seconds later. Most of the smoke exited the chimney during this second event (Fig. 3). Cell continued to glow red hot for several minutes.
Cell B	211	$>425^a$	A single flash flame event which shook the test enclosure; smoke exuded from chimney.
Cell C	274	741	Cell vented fume, which burnt steadily for 22 seconds and self-extinguished. After a further 5 seconds violently re-ignited. Fume/smoke could be seen from the chimney throughout this event.
Cell D	68	743	Cell emitted sparks from positive terminal at venting, followed approximately 2 seconds later by a brief flash fire, and then a gently burn for a further 10 seconds. A dark smoke was expelled from the side of the enclosure during the main event.
Cell E	161	$>515^a$	The cell had no clear sign of venting, but instead underwent a single failure event which caused a flash flame, smoke to be emitted from the sides of the test enclosure as well as the chimney, and the test enclosure to slightly shift on its stand.
Cell F	Not recorded	Not recorded	The vent produced an initial jet of fume, which could be seen exiting the chimney, and then within 1 second changed to a flash flame. This burst open the lid of the enclosure (breaking the closures) emitting fume and flame.
Cell G	179	$>236^a$	Violent event: cell vented with flame, test enclosure rocked, and sparks exited chamber.
Cell H	307	657	Cell vented with a small flame. Smoke seen. 100 seconds later a more vigorous event-smoke, sparks but no prolonged flame.
Cell I	121	>550	Noise of venting, followed shortly (3 secs) by vigorous flame event which forced test enclosure open.

^{a} Thermocouple became detached from cell during the failure event.

smoke particulate matter-lithium both from the cathode structure and the ionic conductor within the electrolyte (most often lithium hexafluorophosphate), aluminium and copper from the current collectors onto which the electrode materials are
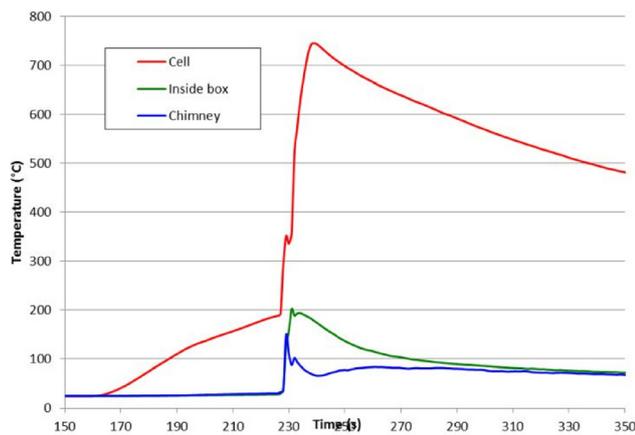
Fig. 4 Temperatures observed during the failure of cell D.

coated, together with nickel, cobalt and manganese from the cathode. The fact that the major components of the smoke originates from the cathode can be assumed from the predominance of nickel, cobalt and manganese within the smoke. The ratio of these three metals as 1:1:1 is consistent with a typical cathode material to be expected in a cell of that generation. The excess of the lithium (at least in mole%) reflects the additional source of lithium from the electrolyte as well as the cathode material.

There is more aluminium from the cathode current collector seen than copper from the anode collector; this is likely to be due to the internal temperature of the cell during failure being hot enough to melt aluminium, making it mobile enough to be carried out of the cell by the exiting gas stream. Such particles of molten aluminium are likely to react with air to form oxides. Copper, with its much higher melting point (1083 °C as compared to 660 °C for aluminium) is less likely to have been released from the cell in this manner. It may be that in failure events involving multiple cells, where which generate higher temperatures, that more significant levels of copper are seen in the smoke and in the residues.

Furthermore, the residues recovered by swabbing the inside of the test box show generally the same materials present, with the notable exception of an increased proportion of aluminium. This is likely to be due to the aluminium exuded from the current collector. If exciting the cells as a fine mist of molten aluminium this is likely to either condense rapidly or react with oxygen to produce an alumina species. These particles would appear to be large enough to settle rapidly within the test chamber rather than being carried within the smoke.

Fig. 7 shows similar results for all the cells under test; here only the materials likely to be within the cathode are shown; small proportions of lithium and copper were generally also seen. Full detail can be found in the ESI.†

These results on the full range of cells tested are similar to those shown in Fig. 6, namely that the metals that form the cathode are also present in the sooty residues and the smoke particulate matter, and in broadly similar ratios, although the proportion of nickel in the smoke particulate seems slightly higher than in the residues.

Note that aluminium, whilst generally seen as a current collector for the cathode is in the NCA chemistry also a component of the cathode. Cells formed with this cathode are most easily distinguished by the lack of manganese in the analysis; cell B within the current set is a clear example of this.

Two of the cells tested here, cells F and G are most likely to use lithium cobalt oxide (LCO, LiCoO$_2$) as the cathode material; for cell G, this was stated within the cell data sheet (it is unusual for cell manufacturers to be precise about their cathode compositions). Although one of the original cathode materials in the first commercial lithium-ion cells, LCO is not now often used, generally only finding uses in high-reliability sectors such as space where 'qualification' of a cell is an onerous task and where performance of a cell is required to be known over a protected timescale.

The remaining cells are all examples of NMC chemistry. The three metals used in the cathode have been varied as advances are made in increasing the cell energy storing capacity (often associated with increasing the proportion of nickel) and decreasing the cost (reducing the cobalt content is an easy way to achieve this).

It is clear that in many of these samples particularly in cells C, D and H, the proportion of aluminium observed in the solid residue is greater than that in the smoke particulate. This is most likely due to the larger sized globules of molten aluminium ejected which will either condense or rapidly react in air to form alumina compounds. Conversely, for cells F and G

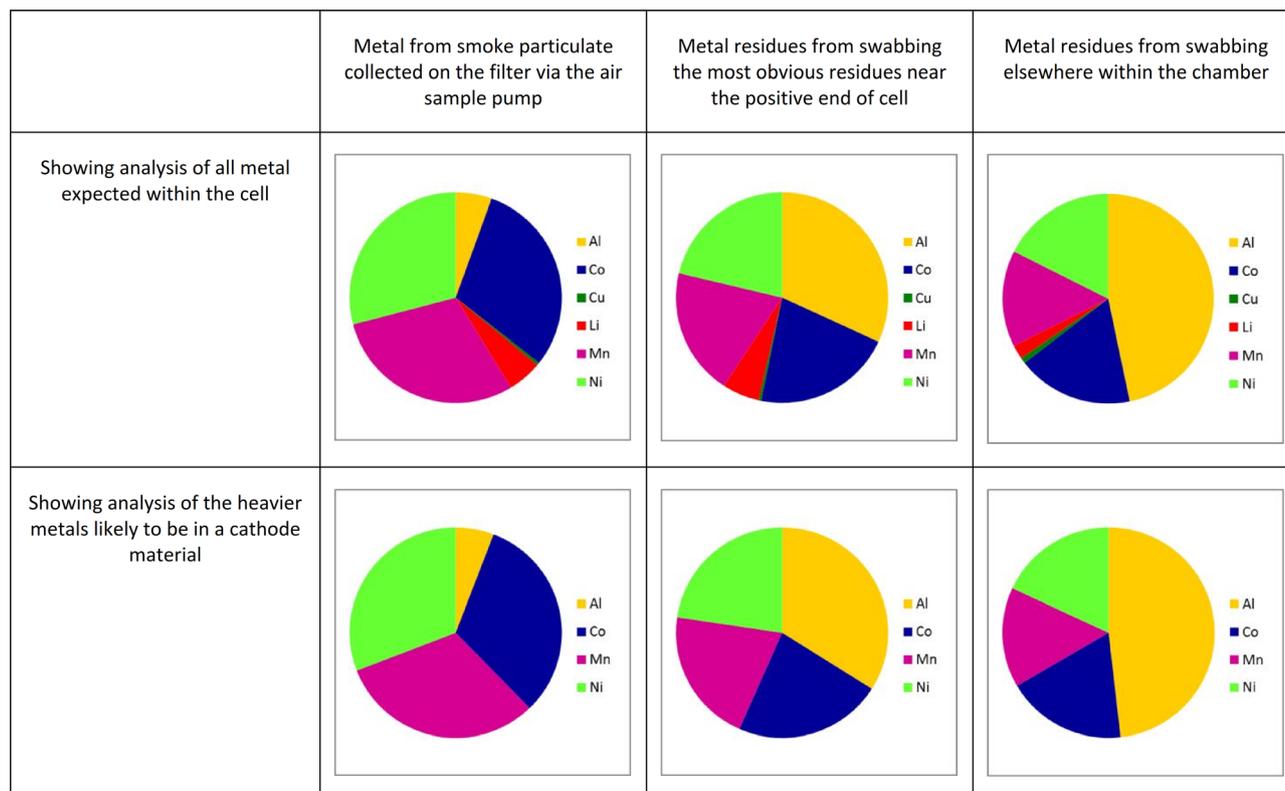Fig. 5 The test chamber before and after a test.

Fig. 6 Proportions of metals observed from samples taken from failure of cell C.

Table 3 Percentage of metals in each sample from cell C

	Metal from smoke particulate collected on the filter *via* the air sample pump		Metal residues from swabbing the most obvious residues near the positive end of cell		Metal residues from swabbing elsewhere within the chamber	
	Mass%	Mole%	Mass%	Mole%	Mass%	Mole%
Lithium	5	30	6	26	2	11
Nickel	29	20	21	12	18	10
Manganese	30	22	19	12	15	9
Cobalt	30	20	21	12	18	10
Copper	0	0	0	0	1	0
Aluminium	5	8	32	38	47	59

there is less aluminium in the residue than the smoke; these cells have an LCO cathode-the higher temperatures generated by this cathode upon failure, and the more violent events observed may suggest that the aluminium is more likely to be widely dispersed when these cells fail.

In cell A, the proportion of cobalt within the residues is significantly more than that within the smoke particulate. Likewise in cell H the proportion of the nickel within the residues is less than that in the smoke particulate. It is possible that some of these cells have 'blended' cathodes; for example, a blend of NMC ($LiNi_xMn_yCo_{(1-x-y)}O_2$) and lithium manganese oxide ($LiMnO_2$) has been used. It may be that in a case like this, one component of the blend has different sized particles, reacts faster or produces particles more likely to be caught up in the smoke rather than deposited as a residue.

The methods of analysis used here do not allow the comprehensive determination of the metal containing compounds/

species; this is the subject of further work. However, it is not unreasonable to expect metal oxides to be formed from a combustion event, and some of the oxides of cobalt, manganese and in particular nickel are known to be hazardous to human health. The health impact of such an exposure depends not only on the species present, but also to the bioavailability of the compounds, influenced by solubility and, for inhaled absorption, particle size. Certainly, initial effects from exposure to the aforementioned metal oxides would present as skin and inhalation irritations. More long-term health effects can include cancer and neurological issues. These compounds would also have a detrimental effect on the environment and the wildlife in surrounding areas.

The potential hazard of such exposures should be taken into account when considering hazards when dealing with batteries after a burning event. It would be possible to evaluate any exposures after an event where battery contents were released;
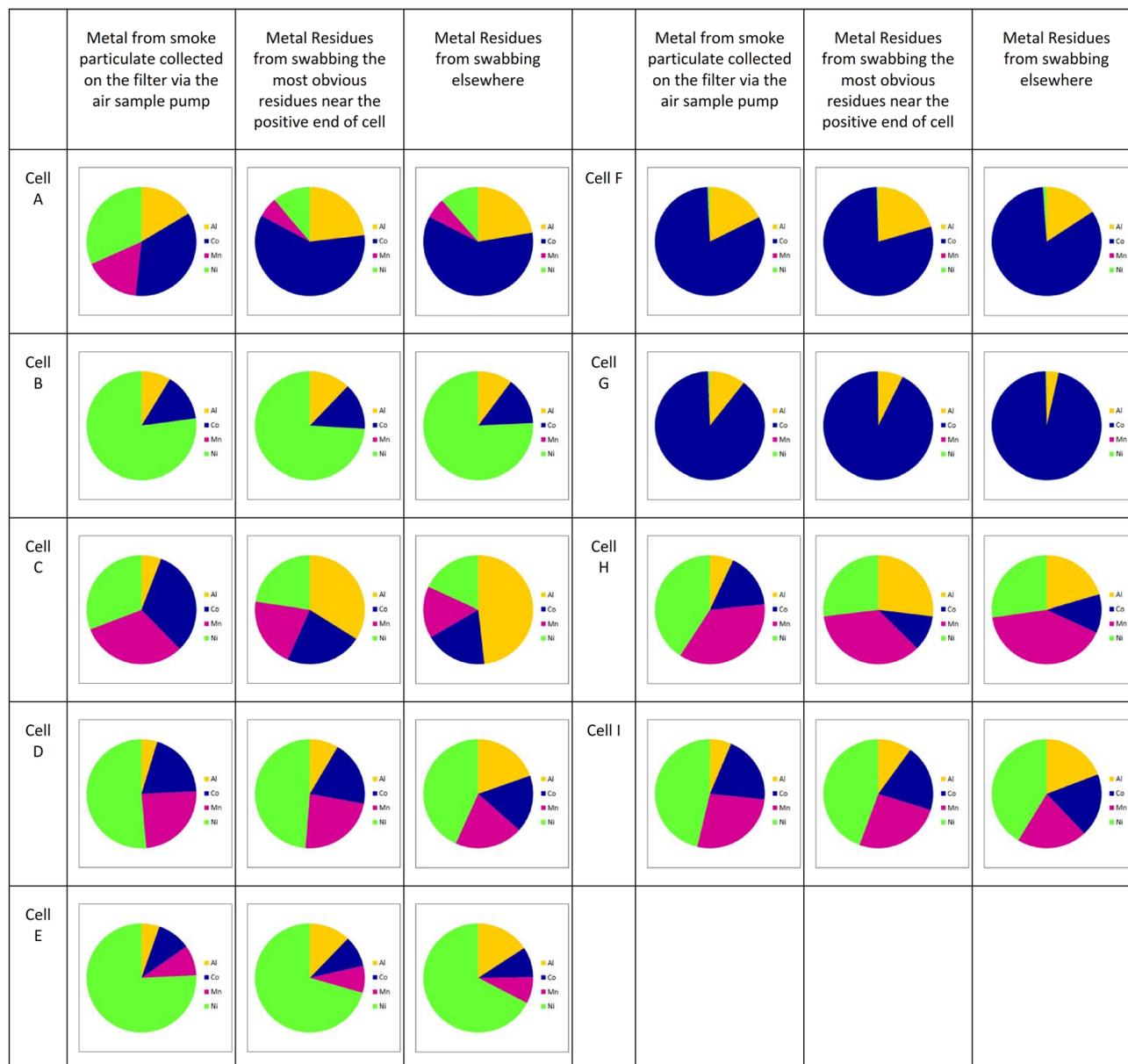
Fig. 7 Cathode metal proportions observed for all cells tested.

this can be done by residue testing for all chemicals or by a direct measurement of exposure in a biological monitoring sample such as urine, where all elements discussed can be determined to confirm exposures. The elimination kinetics would need to be established so that exposure could be captured. Future work will include a more complete/comprehensive analysis, including organic compounds, of the fume captured to better characterise exposures.

Conclusions

Results from this study show that the cathode metals dominate/mimic those seen in the smoke. Subtle differences are observed in the residues and where they are sampled from. These findings suggest that it may be possible to identify the battery devices that have been involved in a fire event. It is also imperative that care is taken when sampling and cleaning residues that remain from any such event.

Furthermore, such a release of smoke may cause a risk to health and the environment, and this should be considered in a fire scenario. Further work will aim to characterise the fume in more detail, investigate different charge states of the batteries, look at the contribution from electronic devices and aim to collect a more representative sample of the plume produced. Therefore, there are still clear outstanding questions relating to the potential toxicology of this smoke or fire residue. Further work is currently being undertaken to continue to probe this.

Author contributions

Jonathan E. H. Buston: Conceptualization, methodology, data curation, writing – original draft, writing – review & editing, visualization, supervision. Jason Gill: investigation, writing – review & editing. Rebecca Lisseman: investigation. Jackie Morton: conceptualization, writing – original draft, writing – review & editing, supervision, funding acquisition. Darren Musgrove: investigation. Rhiannon C. E. Williams: investigation, data curation.

Disclaimer

The contents of this paper, including any opinions and/or conclusions expressed, are those of the authors alone and do not necessarily reflect HSE policy.

Conflicts of interest

There are no conflicts to declare.

Acknowledgements

References

1 M. J. Loveridge, G. Remy, N. Kourra, R. Genieser, A. Barai, M. J. Lain, Y. Guo, M. Amor-Segan, M. A. Williams, T. Amietszajew, M. Ellis, R. Bhagat and D. Greenwood, Looking deeper into the galaxy (Note 7), *Batteries*, 2018, **4**, 1–11.

2 P. Sun, R. Bisschop, H. Niu and X. Huang, A Review of Battery Fires in Electric Vehicles, *Fire Technol.*, 2020, **56**, 1361–1410.

3 R. Bisschop, O. Willstrand, F. Amon and M. Rosengren, Fire safety of lithium-ion batteries in road vehicles, RISE Report 2019:50, 2019.

4 A. Barowy, A. Klieger, J. Regan and M. Mckinnon, *9540A Installation Level Tests with Outdoor Lithium-ion Energy Storage System Mockups*, 2021.

5 Youtube, Video of electric motorbike fire, https://www.youtube.com/watch?v=0uhzlnpjTQk.

6 B. Liu, Y. Jia, C. Yuan, L. Wang, X. Gao, S. Yin and J. Xu, *Energy Storage Mater.*, 2020, **24**, 85–112.

7 J. Garche and K. Brandt, *Electrochemical power sources: Fundamentals, systems, and applications: Li-battery safety*, 2018.

8 F. Larsson, P. Andersson, P. Blomqvist and B. E. Mellander, Toxic fluoride gas emissions from lithium-ion battery fires, *Sci. Rep.*, 2017, **7**, 1–13.

9 K. C. Abbott, J. E. H. Buston, J. Gill, S. L. Goddard, D. Howard, G. Howard, E. Read and R. C. E. Williams, Comprehensive Gas Analysis of a 21700 NMC Li-ion Cell using Mass Spectrometry, *J. Power Sources*, 2022, **539**, 231585.

10 A. W. Golubkov, S. Scheikl, R. Planteu, G. Voitic, H. Wiltsche, C. Stangl, G. Fauler, A. Thaler and V. Hacker, Thermal runaway of commercial 18650 Li-ion batteries with LFP and NCA cathodes – Impact of state of charge and overcharge, *RSC Adv.*, 2015, **5**, 57171–57186.

11 H. Wang, H. Xu, Z. Zhang, Q. Wang, C. Jin, C. Wu, C. Xu, J. Hao, L. Sun, Z. Du, Y. Li, J. Sun and X. Feng, Fire and explosion characteristics of vent gas from lithium-ion batteries after thermal runaway: a comparative study, *eTransportation*, 2022, **13**, 100190.

12 J. Sun, J. Li, T. Zhou, K. Yang, S. Wei, N. Tang, N. Dang, H. Li, X. Qiu and L. Chen, Toxicity, a serious concern of thermal runaway from commercial Li-ion battery, *Nano Energy*, 2016, **27**, 313–319.

13 A. O. Said, C. Lee, S. I. Stoliarov and A. W. Marshall, Comprehensive analysis of dynamics and hazards associated with cascading failure in 18650 lithium ion cell arrays, *Appl. Energy*, 2019, **248**, 415–428.

14 A. W. Golubkov, D. Fuchs, J. Wagner, H. Wiltsche, C. Stangl, G. Fauler, G. Voitic, A. Thaler and V. Hacker, Thermal-runaway experiments on consumer Li-ion batteries with metal-oxide and olivin-type cathodes, *RSC Adv.*, 2014, **4**, 3633–3642.

15 D. Sturk, L. Rosell, P. Blomqvist and A. A. Tidblad, Analysis of li-ion battery gases vented in an inert atmosphere thermal test chamber, *Batteries*, 2019, **5**, 1–17.

16 A. O. Said, C. Lee and S. I. Stoliarov, Experimental investigation of cascading failure in 18650 lithium ion cell arrays: Impact of cathode chemistry, *J. Power Sources*, 2020, **446**, 227347.

17 Y. Zhang, H. Wang, W. Li, C. Li and M. Ouyang, Size distribution and elemental composition of vent particles from abused prismatic Ni-rich automotive lithium-ion batteries, *J. Energy Storage*, 2019, **26**, 100991.

18 Y. Zhang, H. Wang, W. Li and C. Li, Quantitative identification of emissions from abused prismatic Ni-rich lithium-ion batteries, *eTransportation*, 2019, **2**, 100031.

19 S. Chen, Z. Wang and W. Yan, Identification and characteristic analysis of powder ejected from a lithium ion battery during thermal runaway at elevated temperatures, *J. Hazard. Mater.*, 2020, **400**, 123169.

20 C. Essl, A. W. Golubkov, E. Gasser, M. Nachtnebel, A. Zankel, E. Ewert and A. Fuchs, Comprehensive hazard analysis of failing automotive lithium-ion batteries in overtemperature experiments, *Batteries*, 2020, **6**, 30.

21 Y. Wang, H. Wang, Y. Zhang, L. Cheng, Y. Wu, X. Feng, L. Lu and M. Ouyang, Thermal oxidation characteristics for smoke particles from an abused prismatic $Li(Ni_{0.6}Co_{0.2}Mn_{0.2})O_2$ battery, *J. Energy Storage*, 2021, **39**, 102639.

22 L. D. Mellert, U. Welte, M. Tuchschmid, M. Held, M. Hermann, M. Kompatscher, M. Tesson and L. Nachef, *Risk*

minimisation of electric vehicle fires in underground traffic infrastructures, 2020.

23 How dangerous are burning electric cars? https://www.empa.ch/web/s604/brandversuch-elektroauto.

24 T. L. Barone, T. H. Dubaniewicz, S. A. Friend, I. A. Zlochower, A. D. Bugarski and N. S. Rayyan, Lithium-ion battery explosion aerosols: Morphology and elemental composition, *Aerosol Sci. Technol.*, 2021, **55**, 1183–1201.

25 W. T. Luo, S. B. Zhu, J. H. Gong and Z. Zhou, Research and Development of Fire Extinguishing Technology for Power Lithium Batteries, *Proc. Eng.*, 2018, **211**, 531–537.

26 Engie Investigates Source of Belgian Battery Blaze, https://www.greentechmedia.com/articles/read/engie-investigates-source-of-belgian-battery-blaze, (accessed 17 August 2021).

27 D. Hill, *McMicken Battery Energy Storage System Event Technical Analysis and Recommendations*, 2020.

28 M. B. Mckinnon, S. DeCrane and S. Kerber, *Four Firefighters Injured In Lithium-Ion Battery Energy Storage System Explosion - Arizona*, 2020.

29 Tesla, *Model S Emergency response Guide*, 2016.

30 A. Nedjalkov, J. Meyer, M. Köhring, A. Doering, M. Angelmahr, S. Dahle, A. Sander, A. Fischer and W. Schade, Toxic gas emissions from damaged lithium ion batteries-analysis and safety enhancement solution, *Batteries*, 2016, **2**, 1–10.

31 D. E. Schraufnagel, The health effects of ultrafine particles, *Exp. Mol. Med.*, 2020, **52**, 311–317.

32 C. Klein and M. Costa, *Handbook on the Toxicology of Metals*, Fourth Edn, 2015, pp. 1091–1111.

33 B. Sjögren, A. Iregren, J. Montelius and R. A. Yokel, *Handbook on the Toxicology of Metals*, Fourth Edn, 2015, p. 549.

34 R. G. Lucchini, M. Aschner, Y. Kim and M. Šarić, *Handbook on the Toxicology of Metals*, Fourth Edn, 2015, pp. 975–1011.

35 H. A. Roels, R. M. Bowler, Y. Kim, B. Claus Henn, D. Mergler, P. Hoet, V. V. Gocheva, D. C. Bellinger, R. O. Wright, M. G. Harris, Y. Chang, M. F. Bouchard, H. Riojas-Rodriguez, J. A. Menezes-Filho and M. M. Téllez-Rojo, Manganese exposure and cognitive deficits: a growing concern for manganese neurotoxicity, *Neurotoxicology*, 2012, **33**, 872–880.

36 H. Aral and A. Vecchio-Sadus, Toxicity of lithium to humans and the environment-A literature review, *Ecotoxicol. Environ. Saf.*, 2008, **70**, 349–356.

37 K. C. Abbott, J. E. H. Buston, J. Gill, S. L. Goddard, D. Howard, G. Howard, E. Read and R. C. E. Williams, Comprehensive gas analysis of a 21700 $Li(Ni_{0.8}Co_{0.1}Mn_{0.1}O_2)$ cell using mass spectrometry, *J. Power Sources*, 2022, **539**, 231585.